*Available online www.jocpr.com*

**Journal of Chemical and Pharmaceutical Research, 2015, 7(10):295-306**

**Research Article**

**ISSN : 0975-7384**
**CODEN(USA) : JCPRC5**

# Suitable organoclays for removing slightly soluble organics from aqueous solutions

**Nabil Bougdah[1,2]*, Pierre Magri[1], Ali Modaressi[1], Fayçal Djazi[2,4], Rachida Zaghdoudi[3,4] and Marek Rogalski[1]**

*[1]LCP-A2MC, Université de Lorraine, 1, bd Arago-57078 METZ, Cedex 3, France*
*[2]Département de Pétrochimie et Génie des Procédés, Faculté de Technologie, Université 20 Août 1955-Skikda, BP 26 Route d'El-Hadayek, Skikda 21000, Algérie*
*[3]Département Sciences de la matière, Faculté des Sciences, Université 20 Août 1955- Skikda*
*[4]Laboratoire LRPCSI, Université du 20 Août 1955, B.P 26 Skikda 21000, Algérie*

---

**ABSTRACT**

*The adsorption capacity of organo-bentonite towards slightly soluble in water organic compounds of different polarity was studied. The organic solutes were chlorobenzene, toluene and nitrotoluene. The adsorbent were the natural bentonite, the bentonite modified by $Na^+$ ion exchange and organo-bentonites intercalated with hexadecyltrimethyl ammonium, HDTMA, dimethylformamide, DMF, and dimethylsulfoxyde, DMSO. All adsorbent were characterized with the FTIR spectroscopy, XRD and TGA. Experimental results obtained make it possible to acquire a better comprehension of the adsorption mechanism and may be used to improve designing of suitable organo-bentonites for adsorption processes.*

**Keywords**: bentonite, adsorption mechanism, slightly soluble organics, organoclays

---

## INTRODUCTION

The application of natural and modified clays in removing nonionic organic compounds from contaminated environmental water has been extensively studied during last decades due to the high efficiency and low cost of these materials. Special attention was paid to modified bentonites that display interesting sorption properties and are easily intercalated with organic compounds. Modification of bentonites consists on [1–3] replacing the naturally occurring cations (e.g. $Na^+$, $K^+$, and $Ca^{2+}$) in the internal surface of bentonite and removing the hydrating layers of water molecules. The removed water may be replaced by an organic solvent intercalating the interlayer space. It is widely accepted that the sorption to the inner surface of bentonite depends on the type of cation adsorbed [4,5]. Adsorption is enhanced in the presence of weakly hydrated cations ($Cs^+$, $Rb^+$, $K^+$, or $NH^{4+}$), and lowers with strongly hydrated cations ( $H^+$, $Na^+$, $Ca^{2+}$, $Mg^{2+}$, $Al^{3+}$) [4, 6-8]. It was observed that organic cations of certain surfactants such as hexadecyltrimethyl, $HDTMA^+$ [9,10] lowers the hydrophobic character of the interlayer and enhance sorption of organic compounds) from water [1-2, 11-15].

When the interlayer space is filled with an organic solvent the sorption mechanisms corresponds to the solute partitioning between the bulk, aqueous phase and the microscopic organic phase confined in the interlayer space. Nevertheless, the solute retention may occur through adsorption to the surfaces, also. Recent studies [20-23] indicate that the $-NO_2$ groups can form complexes with the weakly hydrated exchangeable cations. In the case of nitroaromatics, the aromatic ring interacts with the hydrophobic portion of clay surfaces enhancing the stability of the complex [23,24,15].

Therefore, a careful analysis of bentonite sorption should take into account various mechanisms [16,17,18,19].

Numerous studies on organobentonite adsorption were published in the literature and various aspects of the adsorption mechanism were studied. It is widely accepted that the bentonite intercalated with $HDTMA^+$ cation is the optimal sorbent of nonpolar organic compounds [25]. In the present study we were concerned with selection of suitable organobentonites to removing slightly soluble aromatic compounds from aqueous solutions. We have been dealing with three substituted benzenes of different polarity: toluene, chlorobenzene and nitrotoluene. Nitrotoluene is highly polar and may form complexes. Two others are weekly polar. All three compounds are fairly soluble in water.

The sorption experiments were carried out with a natural Algerian bentonite, with Na-bentonite and with three organobentonites i.e. HDTMA-bentonite, DMSO bentonite, DMF-bentonite. In spite of the fact that HDTMA-bentonite is considered as optimal adsorbent, we decided to compare the sorption properties of three organoclays. DMSO bentonite and DMF-bentonite are less known materials, but a comparison of different organoclays makes it possible to have a deeper insight into the sorption mechanism.

The comparison of natural bentonite and $Na^+$-bentonite allows to verify the influence of the clay electroneutrality and hydration on sorption properties. The inner layer of bentonite is composed of one octahedral alumina sheet placed between two tetrahedral silica sheets. Bentonite surface is negatively charged due to the isomorphous substitutions of $Al^{3+}$ and $Si^{4+}$ by $Mg^{2+}$ and $Al^{3+}$. This charged imbalance may be equilibrated by ion exchange. When the electrical neutrality is obtained with $Na^+$, which is easily hydrated in presence of the water, than the layer surface is hydrophilic and the bentonite has a low affinity towards nonpolar compounds. The sorption results presented in this work allows verifying this pattern with the Algerian bentonite.

## EXPERIMENTAL SECTION

### Preparation of organo-clay

The natural bentonite used in this study was from Hammam Boughrara (west Algeria). Chemical properties of this clay were studied and published in the literature. The cation exchange capacity (CEC) was found to be 0.90 meq/g [6]. The chemical composition was as follows: $SiO_2$ - 65.2%, $Al_2O_3$ - 17.25%, $Fe_2O_3$ - 2.1%, MgO – 3.1%, CaO - 5%, $Na_2O$ - 3%, $K_2O$ – 1.7%, $TiO_2$ – 0.2%, As – 0.05%, loss of ignition 2.65% [26].

The Na-exchanged form of the bentonite was prepared by stirring 1 M NaCl solution containing a sample of the clay for 24 hours at ambient temperature. Next, the solution was filtered and the clay was washed with distilled water to remove NaCl and other exchangeable cations from the clay. Rinsing was repeated until the negative reaction on $Cl^-$ ions in filtrate was obtained (test with 0.1 M $AgNO_3$) then dried at 70°C [27]. The Na-bentonite was intercalated with cationic surfactant hexadecyltrimethylammonium bromide (HDTMA) in a following way: 200 ml of 4 % of HDTMA aqueous solution was stirred with 20 g Na-bentonite for 48 h [28]. The bentonite separated by filtration was washed with deionized water in order to completely remove bromide (test with 0.1M $AgNO_{3)}$ and then dried at 70°C [29-33]. The intercalation of DMSO or DMF into bentonite was done in a following way: 20 grams of bentonite was stirred with 200 ml of anhydrous DMSO or DMF for 9 days at 70°C. The filtered clay was washed with 25 ml of dioxane and 25 ml of ethanol, and then dried at 110°C [30-32].

### Characterization of modified clays

Modified bentonites were analyzed using thermal analysis (TGA), infra-red analysis (FTIR) and X-ray diffraction. Thermal balance 2050 TGA V5.4A from TA instruments was used to study the thermal decomposition of clays. The characteristic feature of this equipment was that the heating rate was coupled with the mass loss. Therefore, the temperature of the sample temperature was kept constant until the mass loss corresponding to a chemical reaction was completed. The thermal evolution of the raw materials was followed from the room temperature up to 600°C. The average mass of the sample used was of about 20 mg.

Chemical modifications of clays were confirmed by FTIR spectra obtained a spectrometer of Perkin Elmer (Spectrum One FTIR) in the wave number range of 4000-650$cm^{-1}$.

Structural modifications of clays were characterised by X-ray powder diffraction (XRD). The analysis was performed using Bruker diffractometer, model D8 Advance, equipped with a Cu Kα source and a fast detector Lynxeyes (system θ-θ) and working at the monochromatic radiation $K\alpha_1$ wavelength of copper (λ= 1.5406A°). The measured angular field ranged from 2θ = 4 to 15°.

## RESULTS AND DISCUSSION

### Thermogravimetric analyses

Thermal modification of bentonite, Na-bentonite, HDTMA-bentonite, DMSO-bentonite, and DMF-bentonite are illustrated by curves given in fig.1.

TGA records of the bentonite and Na-bentonite are shown in fig.1.a-b. The mass loss of 8.7% and 3% corresponding to the dehydration of these clays were observed respectively at 80.7°C and 75.1°C.

TGA thermal curve corresponding to HDTMA-bentonite, fig.1.c, contains four stages of the masse loss process. The water loss was of 2.2% with the maximum desorption rate was observed at 60.6°C. Next three stages corresponding to the surfactant decomposition were observed at 248.8°C, 283.1°C, and 392.1°C with respective mass losses of 17.6%, 3.7%, and 7.9%. It may be concluded that the surfactant constitutes about 30% of the mass of this organoclay.

In the case of DMSO-bentonite, fig.1.d, the two stages reaction was observed. The first mass loss (1.9% at 52.7°C) corresponding to the release of the adsorbed water was followed by the second one (6.2% at 207.06°C) corresponding to the evaporation of DMSO. Thus the organoclay contained of about 6.2% of DMSO.

A more complex TGA thermal curve, fig.1.e, was observed with DMF-bentonite. The four stages of the mass loss were observed in this case. The water loss was (1.6% at 52.3°C) was followed by DMF evaporation (4.0% at 193.9°C) and two stage decomposition of chemisorbed DMF (1: 2.5% at 320.6°C; 2: 2.3% at 532.9°C). Consequently DMF constituted 8.8% of the mass of this organoclay.

It may be noted that the water content in organo clays was within 1.6% - 2.1%. It was of 3% with Na-bentonite and of 8.7% with natural bentonite. The $Na^+$ cation exchange made diminish the clay hydration ratio.

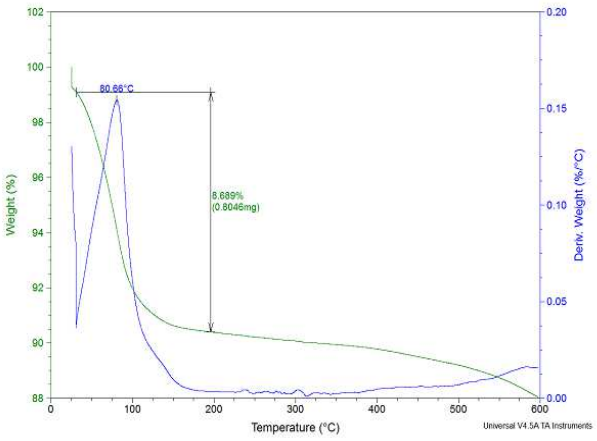


**(a)**

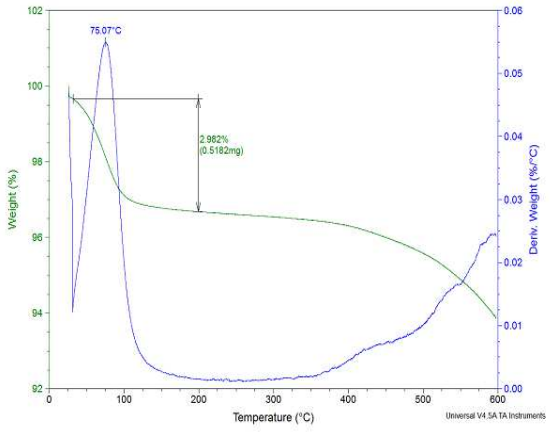


**(b)**

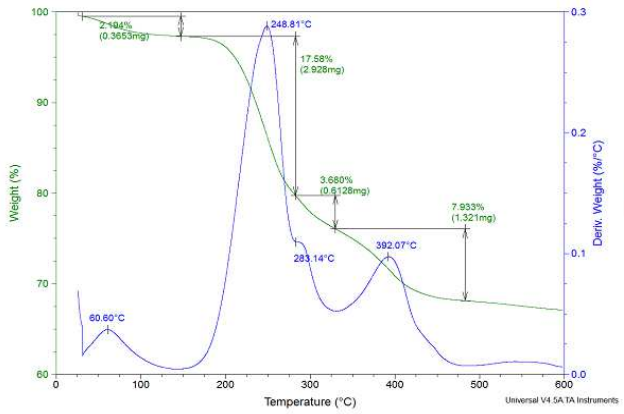


**(c)**

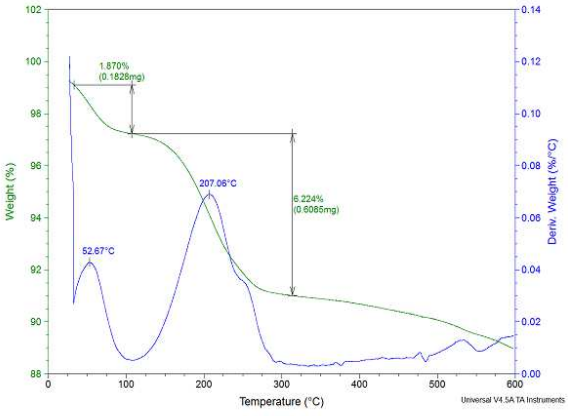


**(d)**

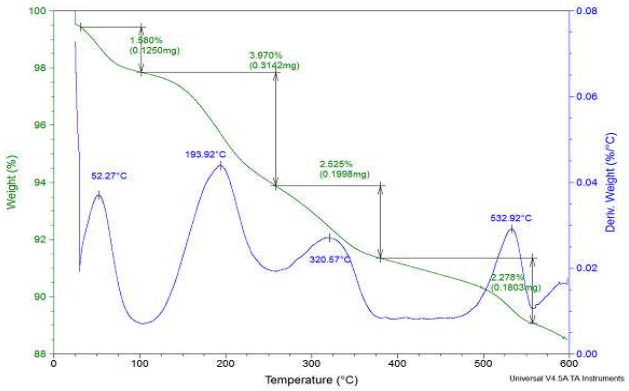


**(e)**

**Fig. 1. TGA/DTG analysis of bentonite (a), Na-bentonite (b), HDTMA-bentonite (c), DMSO-bentonite (d) and DMF-bentonite (e).**

## FT-IR analysis

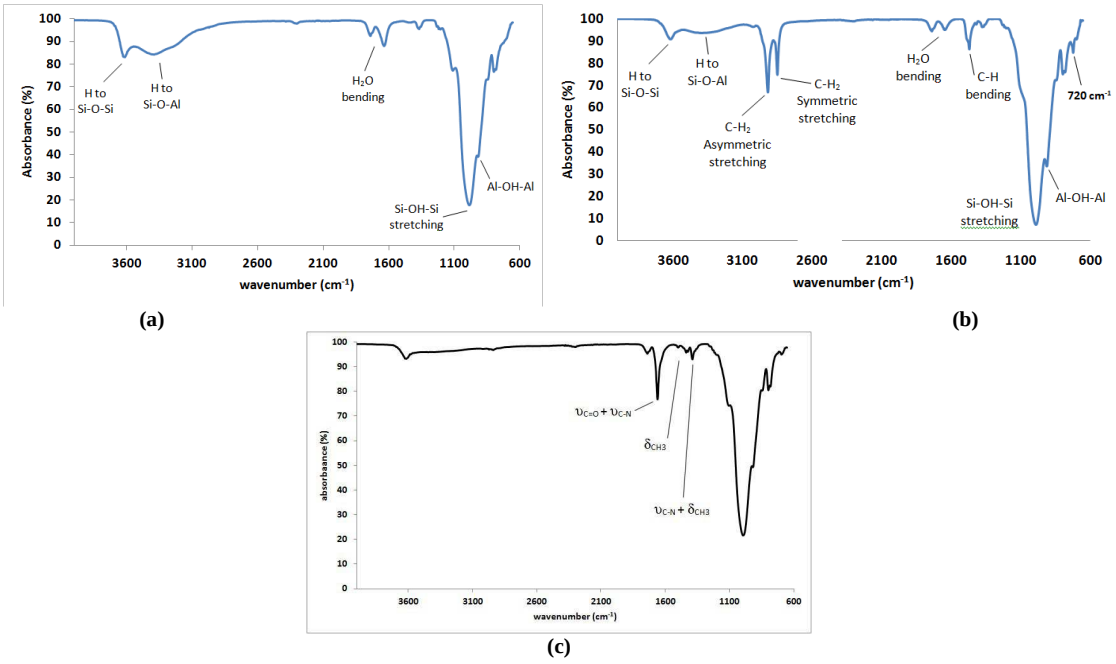


**Fig. 2. Infrared spectra of bentonite (a), HDTMA-bentonite (b) and DMF-bentonite (c)**

Figure 2a displays a typical spectrum of bentonite with the intense band at 982 $cm^{-1}$ from stretching vibration of Si-O, the other bands corresponding to the water sorbed by the clay: the $\upsilon_2$ H-O-H bending vibration spectral range at 1600-1700 $cm^{-1}$; $\upsilon_1$ H-bonding to Si-O-Al is located at 3370-3480 $cm^{-1}$ and the hydrogen bond to Si-O-Si linkage is located at 3613 $cm^{-1}$.

In figure 2b the presence of the HDTMA is confirmed by the significant band at 720 $cm^{-1}$ corresponding to the $CH_2$ rocking mode arosing from the presence of the surfactant.

The band's intensity of the sorbed water decrease with the introduction of HDTMA (1600-1700 $cm^{-1}$ and 3300-3700 $cm^{-1}$), so there is less sorbed water in the modified bentonite. These results are in agreement with the results obtained by TGA.

The introduction of HDTMA increase the vibration stretching band of Si-O-Si from 982 to 988 $cm^{-1}$ and the band of Al-O-Al characteristic for the dioctahedral smectite shifted to lower wavenumbers, here from 916 to 910 $cm^{-1}$. All of our results are in good agreement with the literature [34].

Concerning the HDTMA, the C-H bending band is attributed to a sharp narrow single peak at 1472 $cm^{-1}$ which is associated with a parallel arrangement of the methylene chains at 1468 $cm^{-1}$. The $CH_2$ asymmetric stretching $\upsilon_{as}$ at 2918 $cm^{-1}$ and the symmetric stretching $\upsilon_s$ at 2850 $cm^{-1}$ could be attributed to the gauche trans conformation of the surfactant.

For the DMF-bentonite, the band corresponding to the $\upsilon_{OH}$ is drastically reduced proving the insertion of DMF in the bentonite structure. The chemical function of the DMF is present in the infrared spectra by assigned the well defined band at 1660 $cm^{-1}$ to the $\upsilon_{C=O} + \upsilon_{C-N}$ vibration. The band at 1387 $cm^{-1}$ corresponds to the $\upsilon_{C-N} + \delta_{CH3}$ and the bands between 1400 and 1500 $cm^{-1}$ are attributed to $\delta_{CH3}$.

**XRD analysis**

The XRD spectra of bentonite, Na-bentonite, HDTMA-bentonite, DMSO-bentonite and DMF-bentonite are presented in fig.3 (a), (b), (c), (d) and (e), respectively. Accordingly, the d001 reflection occurs at 2-theta= 6.6 for bentonite, 7.2 for Na-bentonite, 6.3 for DMF-bentonite, 6.3 for DMSO-bentonite and 4.5 for HDTMA-bentonite. This indicates that that the geometry of the interlayer space was modified. The interlayer distance depends on the surface electrical charge and on the arrangement and the nature of molecules filling the interlayer space. The interlayer distance observed in the case of bentonite and Na-bentonite was 13.5 and 12.2 respectively. Natural bentonite surface is negatively charged due to the isomorphous substitutions within the layers of $Al^{3+}$ for $Si^{4+}$ in the tetrahedral sheet and $Mg^{2+}$ for $Al^{3+}$ in the octahedral sheet. When ions on the layer surface are exchanged by $Na^{+}$ the surface is no more charged and the interlayer distance lowers. For modified bentonite the X-ray peak shifted to lower angles indicating increasing basal spacing. In the case of HDTMA-bentonite the interlayer distance was of 1.95 nm. The arrangement of HDTMA molecules in interlayer space depends on the concentration of the surfactant (5, 41-42) going from a monolayer to a bilayer, next, to a pseudo-trimolecular layer and then to a paraffinic quasi crystalline arrangement. The interlayer distance of 1.95 nm corresponds to the bilayer coverage called osmotic domain. A disordered arrangement of the surfactant chains facilitates swelling of organic molecules. For this reason we have selected this material for adsorption experiments. The interlayer distance observed in the case of DMSO-bentonite and DMF-bentonite was of 14.1 nm and 13.9 nm respectively. These polar solvents intercalate bentonite and form probably bilayer structure in the interlayer space. The interlayer distance is slightly higher comparing to water bilayer.

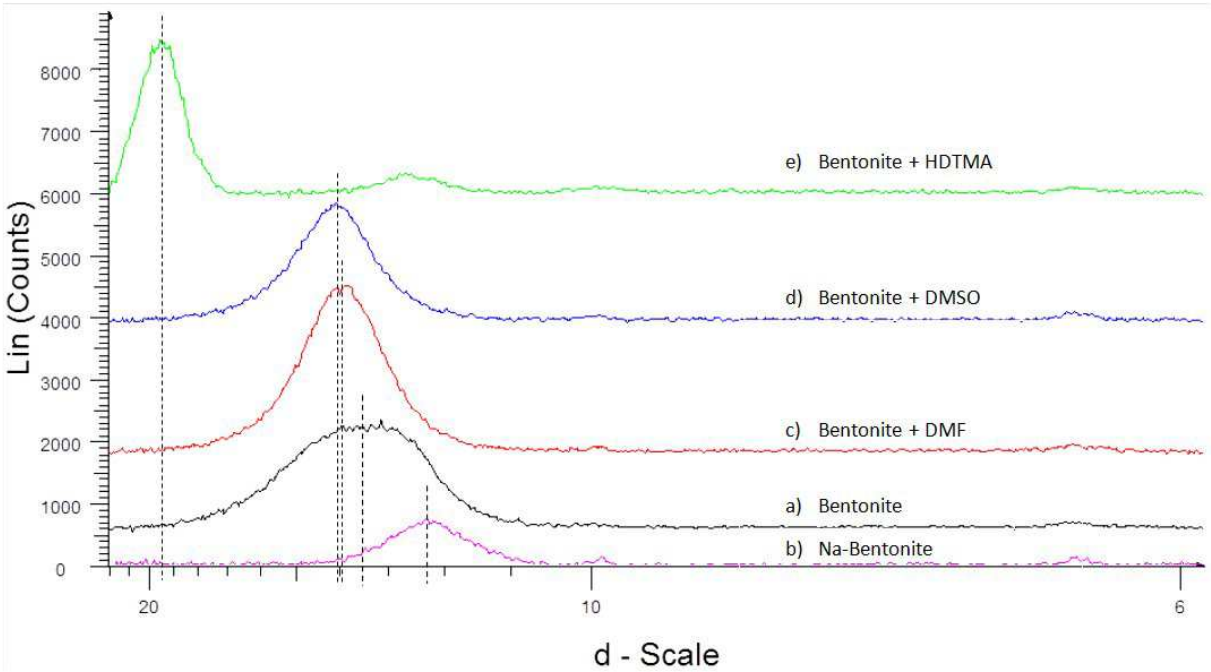


**Fig. 3. XRD pattern of bentonite (a), Na-bentonite (b), HDTMA-bentonite (e), DMSO-bentonite (d) and DMF-bentonite (c)**

**Adsorption kinetics studies**

Kinetic studies of adsorption are helpful to understanding the mechanism of this process. Moreover, the knowledge of adsorption kinetics is important for designing removal of pollutants. In the present study the rates of adsorption of chlorobenzene, toluene and nitrobenzene were determined with bentonite and organobentonites.

Kinetic experiments were carried out in erlenmeyer flasks containing saturated aqueous solutions of chlorobenzene, toluene, or nitrotoluene solutions (100 ml) with 80 mg of the natural bentonite or modified bentonite at 25°C. Solutions were stirred at 300 rpm during selected laps of time. Then, the solution was centrifuged to removing the clay dispersion and analysed using the UV-vis spectrometry. The solution concentration allowed to calculating the quantity $q_t$ (mmol/g) of the organic compound adsorbed by one gram of adsorbent.

$$q_t = (C_0 - C_e) \times \frac{v}{m} \quad (1)$$

Where $q_t$ is the adsorption capacity of the adsorbent, $C_0$ and $C_e$ (mmol/L) are the initial and equilibrium concentrations, respectively, of the adsorbate in the solution. V (L) the volume of the solution and m (g) is the mass of adsorbent used. This experiment was repeated for laps of time going up to 250 min.

Fig.4 presents the adsorption kinetics obtained at room temperature with the initial concentration of adsorbate being 0.25 mmol/L for chlorobenzene and toluene solutions and 0.1458 mmol/L for nitrotoluene solution. The mass of adsorbent was of 80 mg within all experiments.

The mechanism of the adsorption kinetics was studied using two kinetic models.

The first one was the pseudo first-order [15-19], as expressed by the following equation:

$$\mathrm{Log}(q_e - q_t) = \mathrm{Log}(q_e) - (\frac{k_1}{2{,}303}) \times t \quad (2)$$

Where $q_e$ and $q_t$ are the amounts of an organic compound adsorbed at equilibrium and after time t respectively. Rate constant of adsorption was noted as $k_1$ ($min^{-1}$).

If the plot of log ($q_e - q_t$) versus time is linear, then the value of $k_1$ may be directly obtained from the slope.

The pseudo-second order model [20-24] can be written as follows:

$$\frac{dq_t}{dt} = k_2 \times (q_e - q_t)^2 \quad (3)$$

Where $k_2$ is the equilibrium rate constant of the pseudo-second order (g $mmol^{-1}min^{-1}$ or g $mg^{-1}min^{-1}$). Separating variables in eq. (3) and integrating for the boundary conditions $q_t$ =0 to $q_t = q_t$ and t =0 to t = t yields an expression that may be rearranged to the following linear form:

$$\frac{t}{q_t} = \frac{1}{k_2 \times q_e^2} + \frac{t}{q_e} \quad (4)$$

The slope and the intercept allow establishing $q_e$ and $k_2$ respectively.

Parameters of kinetic models together with $R^2$ corresponding to the fit are presented in Tables 1 – 3.

The pseudo-second-order model yields a slightly better fit. Moreover, the value of $q_e$ obtained from the fit is close to the experimental value. The value of $q_e$ obtained with pseudo first order model was almost 100% higher. The fact that the adsorption follows the pseudo-second-order model indicates that adsorbed solutes migrate into the porous structure of the clay. This result agrees with all kinetic studies concerning bentonite and organobentonites.

To have a deeper insight in the mechanism of adsorption the kinetic date were treated with intraparticle diffusion model (IDM) proposed by Weber and Morris [45, 46].

This model is based on expression obtained by solving second Fick's equation for an adsorbent particle suspended in solution:

$$q_t = k_{int} \times t^{\frac{1}{2}} \quad (5)$$

Where $k_{int}$ is the intraparticle diffusion rate constant (mmol/gmin$^{1/2}$ or mg/gmin$^{1/2}$).

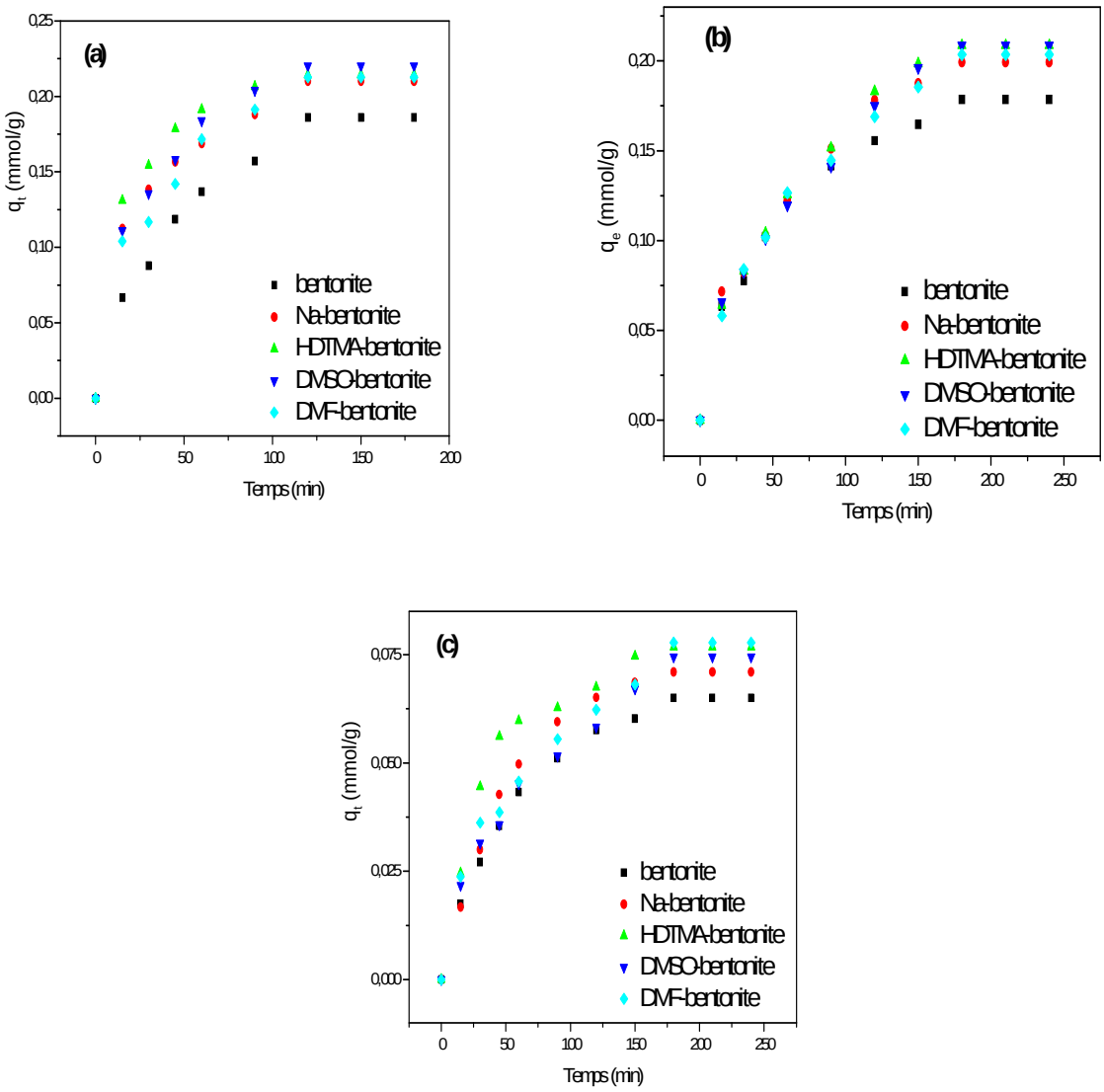


**Fig. 4. Kinetics of adsorption on modified bentonites: a)- chlorobenzene, b)- toluene and c) – nitrotoluene.**

The initial rate of the intraparticle diffusion may be obtained by linearization of this equation as proposed by Wu et al. [47]:

$$\frac{q_t}{q_{ref}} = 1 - R_i\left[1 - \left(\frac{t}{t_{ref}}\right)^{\frac{1}{2}}\right] \qquad (6)$$

Where $R_i = \dfrac{K_p \times t_{ref}^{\frac{1}{2}}}{q_{ref}}$ is defined as a factor of the initial diffusion. If $R_i = 1$ no initial adsorption is observed. If $R_i$ < 0.1 than the initial adsorption is the main process. Therefore, eq.6 makes it possible estimating relative contributions of the initial adsorption and the intraparticle diffusion. $R_i$ may be obtained with the intercept value of eq. (6). According to Mc Key et al. [48] extrapolation of the linear portion of the plot to t = 0 provides intercepts which are proportional to the extent of the boundary layer thickness, that is, the larger the intercept the greater the boundary layer effect retarding IDM. Intercepts indicates the contribution of the initial adsorption in the sorption process.

Fig.5 reports the plots obtained applying kinetic data presented here to eq. 6. It may be observed that the initial adsorption corresponding to intercept is located between 0.9 and 0.5 that corresponds according to Wu at al. [47] to

"intermediately initial adsorption". The highest initial adsorption was observed with chlorobenzene; $R_i$ was of about 0.5 with HDTMA-bentonite and of 0.2 with natural bentonite. The lowest values of $R_i$ observed with toluene were of 0.8 with HDTMA-bentonite and of 0.9 with the natural bentonite. In the case of p-nitrotoluene the intercept value was of about 0.8 with all bentonites and organobentonites. Two conclusions may be drawn. At first, the material displaying the highest initial adsorption is HDTMA-bentonite. Secondly, the lowest values of initial adsorption occurs with nonpolar organics such as toluene.

**Table 1. Pseudo-first order and pseudo-second order kinetics parameters of chlorobenzene adsorption on bentonites**

| Adsorbent | Pseudo-first-order, eq. 2 | | | Pseudo-second-order, eq. 4 | | |
|---|---|---|---|---|---|---|
| | $k_1$ ($min^{-1}$) | $q_e$ calc (mmol/g) | $R^2$ | $k_2$ ($gmmol^{-1}$ $min^{-1}$) | $q_e$ calc (mmol/g) | $R^2$ |
| Bentonite | 0.0195 | 0.4572 | 0.9971 | 0.0961 | 0.2376 | 0.9951 |
| Na-bentonite | 0.0196 | 0.4132 | 0.9995 | 0.2040 | 0.2368 | 0.9984 |
| HDTMA-bentonite | 0.0319 | 0.4351 | 0.9970 | 0.3401 | 0.2320 | 0.9995 |
| DMSO-bentonite | 0.0260 | 0.4722 | 0.9939 | 0.1759 | 0.2522 | 0.9983 |
| DMF-bentonite | 0.0229 | 0.4679 | 0.9867 | 0.1402 | 0.2510 | 0.9961 |

**Table 2. Pseudo-first order and pseudo-second order kinetics parameters of toluene adsorption on bentonites.**

| Adsorbent | Pseudo-first-order, eq. 2 | | | Pseudo-second-order, eq. 4 | | |
|---|---|---|---|---|---|---|
| | $k_1$ ($min^{-1}$) | $q_e$ calc (mmol/g) | $R^2$ | $k_2$ ($gmmol^{-1}$ $min^{-1}$) | $q_e$ calc (mmol/g) | $R^2$ |
| Bentonite | 0.0158 | 0.4402 | 0.9978 | 0.1017 | 0.2159 | 0.9976 |
| Na-bentonite | 0.0183 | 0.5030 | 0.9882 | 0.0728 | 0.2507 | 0.9937 |
| HDTMA-bentonite | 0.0192 | 0.5355 | 0.9788 | 0.0588 | 0.2707 | 0.9940 |
| DMSO-bentonite | 0.0170 | 0.5242 | 0.9675 | 0.0525 | 0.2753 | 0.9894 |
| DMF-bentonite | 0.0149 | 0.4896 | 0.9921 | 0.0597 | 0.2626 | 0.9959 |

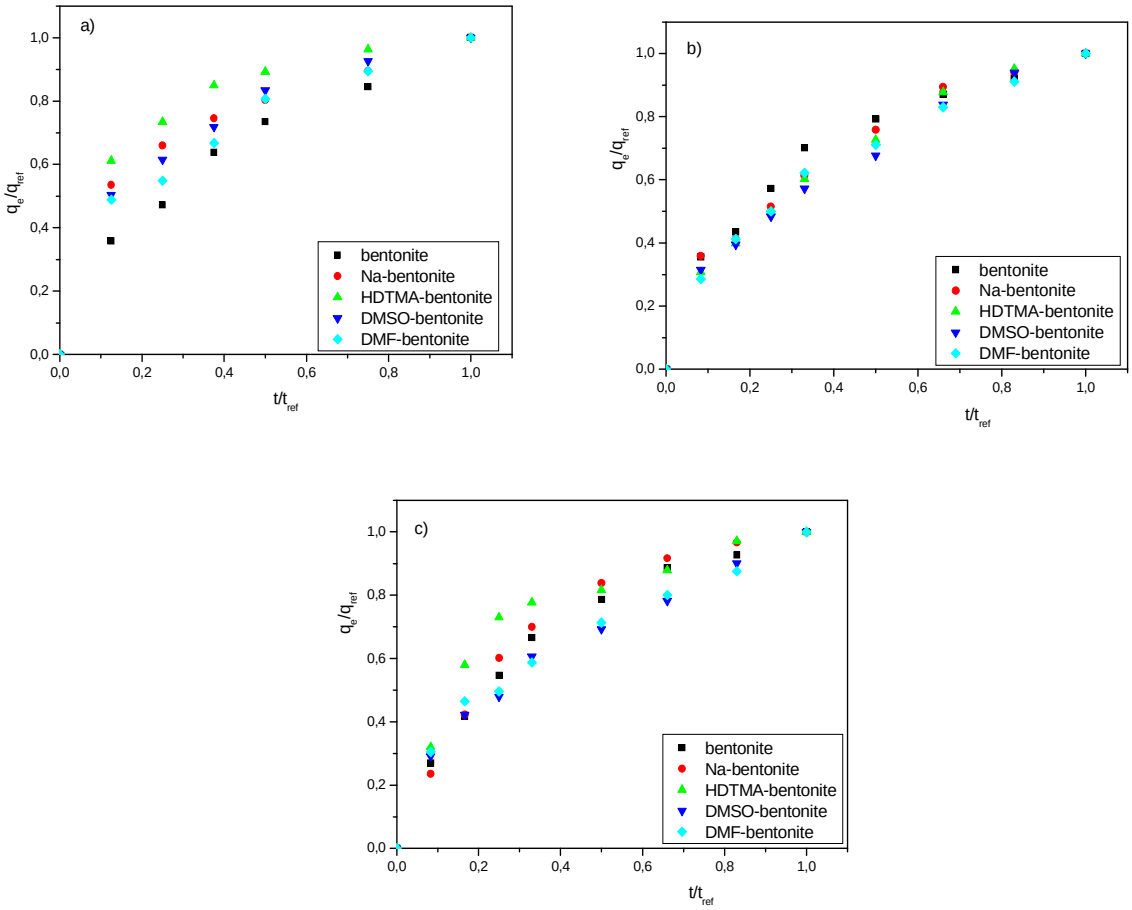


**Fig. 5. Adsorption characteristic curves of the dimensionless IDM: a)- chlorobenzene, b)- toluene and c) – nitrotoluene**

**Table 3. Pseudo-first order and pseudo-second order kinetics parameters of nitrotoluene adsorption on bentonites.**

| Adsorbent | Pseudo-first-order, eq. 2 | | | Pseudo-second-order, eq. 4 | | |
|---|---|---|---|---|---|---|
| | $k_1$ ($min^{-1}$) | $q_e$ calc (mmol/g) | $R^2$ | $k_2$ ($gmmol^{-1}$ $min^{-1}$) | $q_e$ calc (mmol/g) | $R^2$ |
| Bentonite | 0.0172 | 0.3006 | 0.9990 | 0.2146 | 0.0825 | 0.9982 |
| Na-bentonite | 0.0225 | 0.3349 | 0.9975 | 0.2093 | 0.0895 | 0.9955 |
| HDTMA-bentonite | 0.0196 | 0.3010 | 0.9567 | 0.3554 | 0.0883 | 0.9981 |
| DMSO-bentonite | 0.0134 | 0.3115 | 0.9823 | 0.1563 | 0.0963 | 0.9925 |
| DMF-bentonite | 0.0123 | 0.3057 | 0.9964 | 0.1676 | 0.0982 | 0.9928 |

**Adsorption isotherms**

An adsorption isotherm describes the mechanism of retention of the solution components to a solid-phase at a constant temperature and pH. Adsorption equilibrium is established when the ratio between the adsorbed amount with the remaining in the solution becomes constant. The graphical representation of adsorption isotherms provides an insight into the adsorption mechanism, as well as the affinity of the adsorbate/adsorbent couple. Usually, mathematical correlation of adsorption isotherm parameters yields an important tool towards the analysis of the adsorption mechanism.

The adsorption isotherms of toluene, chlorobenzene and nitrotoluene on bentonites and organobentonites were assessed using the same experimental setup as with kinetic experiments. In each experiment a sample of 80 mg of adsorbent (bentonite or modified bentonite) was equilibrated during 3 hours at 25°C with 100 ml of aqueous solutions of toluene or chlorobenzene or nitrotoluene of initial concentrations, $C_{0,}$ between 0.01 and 1 mmol/l.
Results obtained for chlorobenzene, toluene and nitrotoluene are presented in figs 6a, 6b and 6c respectively.

It should be noted that Algerian bentonites and organo-bentonites adsorb higher amounts of toluene and chlorobenzene as compared to bentonites of different origins described in the literature. The retention of the organic solutes on different clay materials at equilibrium was compared at the solute concentration of $C_e = 0.15$ (mmol/L) for all solutes and materials studied. It was observed that the retention of nitrotoluene was of 0.086, 0.099, 0.105, 0.109 and 0.112 mmol/g for bentonite, Na-bentonite, DMSO-bentonite, HDTMA-bentonite and DMF-bentonite, respectively. The retention of toluene was of 0.293, 0.414, 0.465, 0.465 and 0.497 mmol/g for bentonite, Na-bentonite, DMF-bentonite HDTMA-bentonite and DMSO, respectively and the retention of chlorobenzene was of 0.361, 0.43, 0.437, 0.477 and 0.728 mmol/g for bentonite, DMF-bentonite, Na-bentonite, HDTMA-bentonite and DMSO-bentonite, respectively.

DMSO-bentonite is the most efficient material to removing toluene and chlorobenzene (particularly chlorobenzene) and DMF-bentonite is the best adsorbent for nitrotoluene. Na-bentonite is better adsorbent than natural bentonite and the retention observed with this clay was only slightly lower than with HDTMA-bentonite adsorbent.

Results obtained confirm the idea that elaborating organoclays one should have in mind the chemical affinity between solute, bentonite and intercalated organic compound [25]. Indeed, the uptake of organic solutes may be doubled if the interlayer space is filled with a suitable solvent.

The shape of adsorption isotherms gives some indications concerning the adsorption mechanism. In the case of toluene and chlorobenzene the adsorption is negligible for solution concentration lower than a critical threshold being of 0.05 (mmol/L) with chlorobenzene and 0.07 (mmol/L) with toluene. This confirms the cooperative character of adsorption. Kinetic studies showed that in the case of these solutes initial sorption is negligible and that the internal adsorption governed by diffusion is the main process. The adsorption isotherms are linear at higher concentrations. This indicates that the retention mechanism may by reduced to a thermodynamic partition of the solute between the bulk solution and the solvent filling the interlayer space. The solute retention may be expressed by:

$$q_e = q_t + k(c_e - c_t) \qquad (7)$$

where $q_t$ and $c_t$ correspond to the retention and concentration at the critical threshold, and k [L/g] is partition coefficient of the solute between the bulk solution and the solvent filling the interlayer space.
Parameters of eq. 7 are given in Table 4.

**Table 4. Characteristic parameters of IDP**

| | Chlorobenzene | | | Toluene | | | Nitrotoluene | | |
|---|---|---|---|---|---|---|---|---|---|
| | $q_t$ | $c_t$ | k | $q_t$ | $c_t$ | k | $q_t$ | $c_t$ | k |
| Bentonite | 0.127 | 0.078 | 3.243 | 0.175 | 0.104 | 2.549 | 0.047 | 0.072 | 0.492 |
| Na- bentonite | 0.124 | 0.058 | 3.397 | 0.206 | 0.09 | 3.472 | 0.057 | 0.071 | 0.536 |
| HDTMA-bentonite | 0.08 | 0.046 | 3.811 | 0.207 | 0.083 | 3.855 | 0.065 | 0.068 | 0.537 |
| DMSO-bentonite | 0.112 | 0.051 | 6.222 | 0.198 | 0.082 | 3.396 | 0.064 | 0.072 | 0.536 |
| DMF-bentonite | 0.097 | 0.052 | 3.399 | 0.222 | 0.086 | 3.787 | 0.069 | 0.072 | 0.555 |

Kinetic studies demonstrated that the initial adsorption of nitrobenzene is significant and constitutes about 40% of the total adsorption. This observation was confirmed by the pattern of the adsorption isotherm that present a Langmuir like shape at concentrations lower than 0.1 [mmol/L].

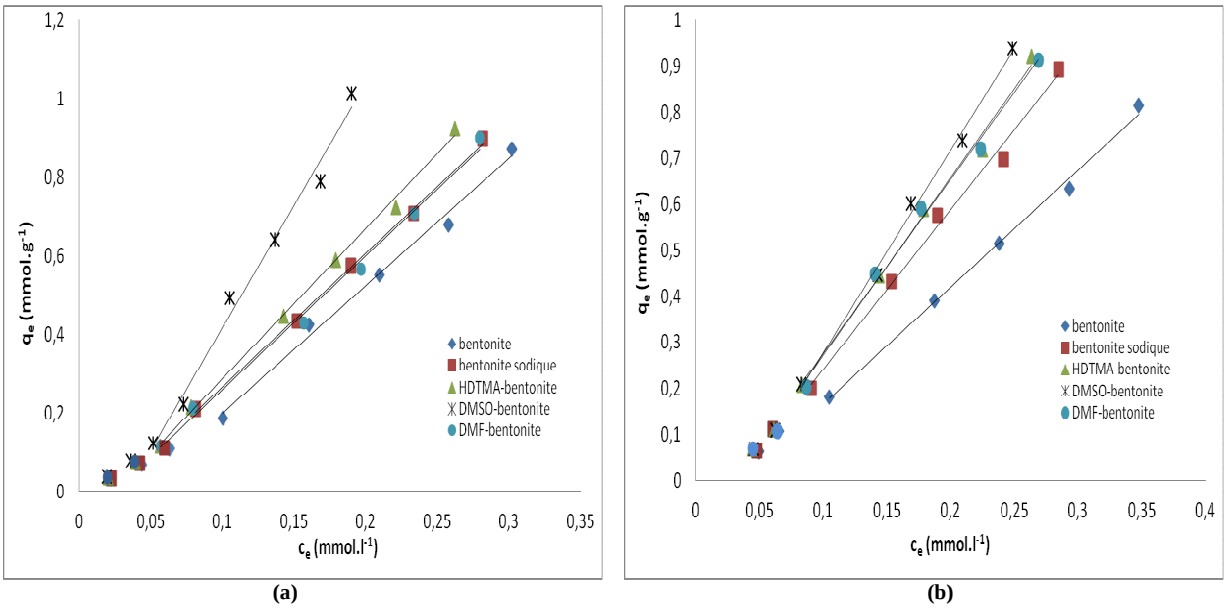


**(a)** **(b)**

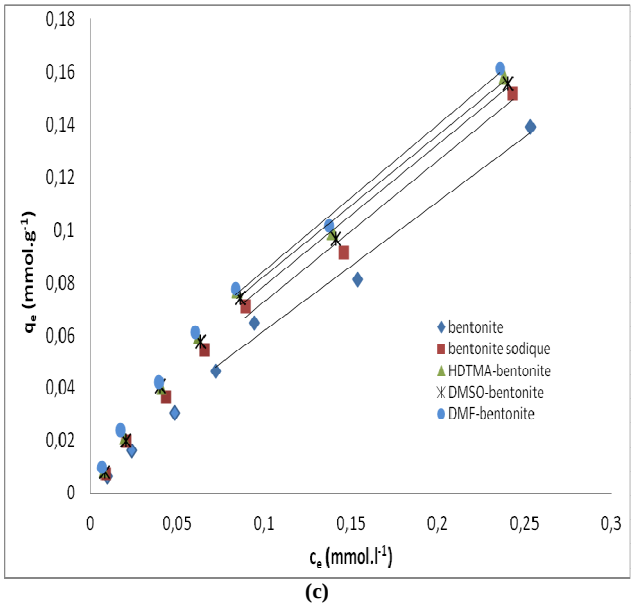


**(c)**

**Fig. 6. Adsorption isotherms of chlorobenzene (a), toluene (b) and nitrotoluene (c) onto different modified bentonite**

## CONCLUSION

Results obtained confirm the utility of modified bentonites to removing slightly soluble organics from aqueous solutions. It was demonstrated that the adsorption mechanism depends on the solute polarity. In the case of toluene, $\mu$ = 0.34 D, adsorption is mainly driven by diffusion, and is negligible at very low concentrations. In the case of nitrotoluene, $\mu$ = 4.44 D, the contribution of the external adsorption that follows the Langmuir pattern is significant.

The highest retention was obtained with modified bentonites using polar solvents; DMSO-bentonite was the best solvent for chlorobenzene and toluene and DMF–bentonite for nitrotoluene. Results obtained with HDTMA-bentonite were only slightly lower with toluene and nitrotoluene but the difference was significant with chlorobenzene. It should be noticed that Na-bentonite, cheap and easily produced material, displays with toluene, chlorobenzene and nitrotoluene quite good adsorption capacity. These results indicate that the adsorption capacity towards a given solute depends on the solvent used to modifying the bentonite. The adsorption capacity depends also on the origin of the bentonite used. It was demonstrated that the Algerian bentonite is good adsorbant.

**Acknowledgments**
The authors are thankful to Ms L. Garoux for X-ray spectra recording and to Dr. S. Rup for FTIR experiments. N. Bougdah thanks The Ministry of Higher Education and Research of Algerian Republic for financial support.

## REFERENCES

[1] S Xu; G Sheng; SA Boyd, *Adv. Agron*., **1997**, 59, 25–62.
[2] J Ma; L Zhu, *J Hazard. Mater*., **2006**, 136(3), 982–988.
[3] J Wagner; H Chen; BJ Brownawell; JC Westall, *Environ. Sci. Technol*., **1994**, 28(2), 231–237.
[4] R Zhu; J Zhao; F Ge; L Zhu; J Zhu; Q Tao; H He, *applied clay science*., **2014**, 88-89, 73–77.
[5] H Li; TR Pereira; BJ Teppen; DA Laird; CT Johnston; SA Boyd, *Environ. Sci. Technol*., **2007**, 41(4), 1251–1256.
[6] A El Messabeb-Ouali; M Benna-Zayani; M Ayadi-Trabelsi; S Sauvé, *international journal of chemistry*, **2013**, 5(2), 12–28.
[7] S Charles; BJ Teppen; H Li; DA Laird; SA Boyd, *Soil Sci. Soc. Am. J*., **2006**, 70(5), 1470–1479.
[8] SA Boyd; G Sheng; BJ Teppen; CT Johnston. Environ, *Sci. Technol*., **2001**, 35(21), 4227–4234.
[9] G Lagaly, *Clay Miner*., **1981**, 16, 1–21.
[10] SA Boyd; J F Lee; MM Mortland, *Nature*., **1988**, 333, 345–347.
[11] L Zhu; B Chen; X Shen. Environ, *Sci. Technol*., **2000**, 34(3), 468–475.
[12] L Zhu; B Chen, *Environ. Sci. Technol*., **2000**, 34(4), 2997–3002.
[13] G Sheng; X Wang; S Wu; SA Boyd, *J. Environ. Qual*., **1998**, 27, 806–814.
[14] B Chen; L Zhu, *J. Environ. Sci*., **2001**, 13(2), 129–136.
[15] L Zhu; X Ren; S Yu, *Environ. Sci. Technol*., **1998**, 32 (21), 3374–3378.
[16] ER Kinkead; RE. Wolfe; CD Flemming; DJ Caldwell; CR Miller; GB Marit, *Toxicol. Industrial Health*., **1995**, 11(3), 309-323.
[17] JA Smith; PR Jaffe; CT Chiou, *Environ. Sci. Technol*., **1990**, 24(8), 1167–1172.
[18] G Sheng; S Xu; SA Boyd, *Water Res*., **1996**, 30, 1483–1489.
[19] G Sheng; S Xu; SA Boyd, *Environ. Sci. Technol*., 1996, 30(6), 1553–1557.
[20] SB Haderlein; RP Schwarzenbach, *Environ. Sci. Technol*., **1993**, 27(2), 316-326.
[21] G Sheng; CT Johnston; B J Teppen; S A Boyd, *Clays Clay Miner*., **2002**, 50(1), 25-34.
[22] SB Haderlein; KW Weissmahr; RP Schwarzenbath, *Environ. Sci. Technol*., **1996**, 30(2), 612-622.
[23] SA Boyd; G Sheng; BJ Teppen; CT Johnston. Environ, *Sci. Technol*., **2001**, 35(21), 4227-4234.
[24] CT Johnston; G Sheng; BJ Teppen; SA Boyd; MF De Oliveira, *Environ. Sci. Technol*., **2002**, 36(23), 5067-5074.
[25] B Erdem; AS Ozca; A Ozcan, *Surf. Interface Anal*., **2010**, 42(6-7), 1351–1356.
[26] B Benguella; A Yacouta-Nour, *Desalination*., **2009**, 235(1-3), 276-292.
[27] A Safa Ozcan; Bilge Erdem; Adnan Ozcan, *J colloide and interface science*., **2004**, 280(1), 44-54.
[28] S Al-Asheh; F Banat; L Abu-Aitah, *Separation and Purification Technology*., **2003**, 33(1), 1-10.
[29] Yun Huang; Xiaoyan Ma; Guozheng Liang; Hongxia Yan, *Chemical Engineering Journal*., **2008**, 141(1-3), 1-8.
[30] JJ Tunney; CC Detellier, *J. Clay Minerals*., **1994**, 42(4), 473-476.
[31] JJ Tunney; C Detellier, *J. Chem. Mater*., **1996**, 8, 927-935.
[32] RL Frost; J Kristof; E Horvath; JT Kloprogge, *Thermochimica Acta*., **1999**, 327(1-2), 155-166.
[33] O Ceyhan; H Guler; R Guler, *J. Adsorption Sci &Technol*., **1999**, 17(6), 469-477.
[34] W Xue; H He; J Zhu; P Yuan, *Spectrochimica Acta Part A : molecular and biomolecular spectroscopy*., **2007**, 67(3), 1030-1036.
[35] YS Ho; CC Chiang, *Adsorption*., **2001**, 7(2), 139- 147.
[36] Z Bouberka; S Kacha; M Kameche; S Elmaleh; Z Derriche, *J. Hazard. Mater*., **2005**, 119(1-3), 117–124.
[37] G Chen; B Han; H Yan, *J. Colloid Interface Sci*., **1998**, 201(2), 158–163.
[38] L Yan; X Shan; B Wen; S Zhang, *J. Colloid Interface Sci*., **2007**, 308(1), 11–19.
[39] I Sharma; D Goyal, *J. Sci. Ind. Res*., **2009**, 68(7), 640–646.
[40] S Ho; G Mckay, *Adsorp. Sci. Technol*., **1989**, 16(4), 243–255.
[41] V Ponnusami; R Aravindhan; N Karthik Raj; G Ramadoss; SN Srivastava, *J. Environ. Prot. Sci*., **2009**, 3, 1–10.

[42] S Liang; X Guo; N Feng; Q Tian, *J. Hazard. Mater*., **2010**, 174(1-3), 756–762.
[43] PH Li; RL Bruce; MD Hobday, *J. Chem. Technol. Biotechnol*., **1999**, 74(3), 55-59.
[44] K Shakir; HF Ghoneimy; AF Elkafrawy; ShG Beheir; M Refaat, *J. Hazardous Materials*., **2008**, 150(3), 765-773.
[45] WJ Weber; JC Morris, *in: proceedings of 1st International Conference on Water Pollution Symposium, Pergamon Press, Oxford*., **1962**, vol. 2, 231-266.
[46] WJ Weber; JC Morris, *J. Sanit. Eng. Div. Am. Soc. Civ. Eng*., **1963**, 89(SA2), 31-59.
[47] Feng-Chin Wu; Ru-Ling Tseng; Ruey-Shin Juang, *Chemical Engineering journal*., **2009**, 153(1-3), 1-8.
[48] G McKay; MS Otterburn; AG Sweeney, *Water Res*., **1980**, 14(1), 15-20.
[49] Y Shu; L Li; Q Zhang; H Wu, *J. Hazard. Mater*., **2010**, 173(1-3), 47-53.
[50] S Bedin; MF Oliveira; MGA Vieira; OAA dos Santos; MCG da Silva, *Chem. Eng. Trans*., **2013**, 32, 313-318.

**Nomenclature**

| | |
|---|---|
| HDTMA | Hexadecyltrimethyl ammonium cation. |
| DMF | Dimethylformamide. |
| DMSO | Dimethylsulfoxyde. |
| CEC | Cation exchange capacity. |
| $q_t$ | adsorption capacity of the adsorbent (mmol/g). |
| $C_0$ | Initial concentration (mmol/L). |
| $C_e$ | Equilibrium concentration (mmol/L). |
| $k_1$ | Rate constant of adsorption ($min^{-1}$). |
| $k_2$ | The equilibrium rate constant of the pseudo-second order ($g.mmol^{-1}.min^{-1}$). |
| $R^2$ | Correlation coefficient. |
| $c_t$ | Concentration at the critical threshold. |
| k | Partition coefficient of the solute between the bulk solution and the solvent filling the interlayer space (L/g). |
| IPD | Intraparticle diffusion model. |